

Measuring the equation of state of the universe: Pitfalls and prospects

Irit Maor,¹ Ram Brustein,¹ Jeff McMahon,² and Paul J. Steinhardt²

¹*Department of Physics, Ben Gurion University, Beer-Sheva 84105, Israel*

²*Department of Physics, Princeton University, Princeton, New Jersey 08540*

(Received 21 December 2001; published 31 May 2002)

We explore various pitfalls and challenges in determining the equation of state (w) of the dark energy component that dominates the universe and causes the current accelerated expansion. We demonstrated in an earlier paper the existence of a degeneracy that makes it impossible to resolve well the value of w or its time derivative with supernovae data. Here we consider standard practices, such as assuming that w is constant or greater than -1 , and show that they also can lead to gross errors in estimating the true equation of state. We further consider combining measurements of the cosmic microwave background anisotropy and the Alcock-Paczynski test with supernovae data and find that the improvement in resolving the time derivative of w is marginal, although the combination can constrain its present value perhaps to 20% uncertainty.

DOI: 10.1103/PhysRevD.65.123003

PACS number(s): 98.62.Py, 98.80.Es

I. INTRODUCTION

Measurements of type IA supernovae have shown that the expansion of the universe is accelerating [1,2], suggesting that most of the energy density of the universe consists of some form of dark energy with negative pressure [3]. Combining measurements of the cosmic microwave background anisotropy and observations of large-scale structure provides important corroborating evidence [4,5]. Two candidates for the dark energy are a cosmological constant (or vacuum density) and quintessence [6], a time-varying, spatially inhomogeneous component. In a previous paper [7] (paper I), we addressed the question of whether supernova measurements can be used to measure the equation of state (EOS) of the negative pressure component, the ratio w of the pressure to the energy density. The issue is important because $w = -1$ for a cosmological constant whereas w takes on different values and can be significantly time varying in the case of quintessence [6,8,9]. Under the assumption that w is constant, its value can be determined to better than 5 percent by measuring several thousand supernovae distributed equally between redshift $z=0$ and $z=2$. However, we showed that a degeneracy opens up if w is time-dependent which makes it impossible to determine accurately the current value of w or its time derivative. The cause of the degeneracy is that supernovae measure luminosity distance, which is related by a multi-integral expression to the EOS as a function of redshift, $w(z)$. Widely different $w(z)$ can have the same multi-integral value.

The purpose of this paper is to explore some pitfalls and challenges in determining the EOS and its time variation using supernovae. For example, we shall show how the standard practice of considering only models with $w \geq -1$ or only models with constant w when doing likelihood analyses can lead to grossly incorrect results. For example, we will illustrate cases where the standard practice will suggest that w is near -1 or much more negative than -1 when, in fact, w is significantly greater than -1 and rapidly time varying. We shall show that a nonzero value of dw/dz is more easily detected if $dw/dz > 0$ than if $dw/dz < 0$. We shall also contrast measuring w for the negative pressure component alone

(w_Q) versus the mean value for the total energy density (including ordinary and dark matter), w_T . The degeneracy problem is less severe for w_T , but this parameter provides less useful information. We consider possibilities of breaking the degeneracy between w and dw/dz by combining supernovae results with either cosmic microwave background anisotropy measurements and/or the Alcock-Paczynski test. We shall show that neither additional test significantly improves the measurement of the time variation of w , although optimistic assumptions about the Alcock-Paczynski test suggest that the current value of w can be measured to within 20% or so.

We conclude that a new, yet to be found test has to be devised to resolve well the cosmic EOS and its time variation. We stress that with current data it is possible to determine the EOS to about a factor of two. For a future experiment to significantly enhance the determination of the EOS, and enable the distinction between a constant EOS and a time-dependent one, it needs to resolve the equation of state at the 10% level or better.

The results of our analysis agree with many other analyses [10–22], although not always with their interpretation, and can be used to explain why some other analyses seem to indicate a superior resolving power of SN measurements alone [23–26], or in combination with other measurements [27–30]. Some of the latter analyses implicitly assume unrealistic accuracy in independent determination of cosmological parameters, by not including self-consistently the uncertainty in $w(z)$ in all measurements. For example, assume a reported resolution of matter energy density which was based on assuming $w_Q = -1$, or assume $w_Q > -1$ as a prior.

Type IA supernovae have intrinsic variability of about 0.15 in absolute magnitude, but currently the errors in measuring distant SN are above this. There are ongoing programs to extend the search to deeper redshifts and improve measurement quality. The proposed SNAP satellite plans to measure 2000 SN per year, mostly in the range of redshifts $0.1 < z < 1.2$, and some as far as $z = 1.7$ [31]. The anticipated error in individual magnitudes is $\Delta m = 0.15$ statistical and 0.02 systematic error, which yields about 1% relative error in luminosity distance d_L .

For our numerical estimates, we have generated 50 SN magnitudes randomly chosen from a uniform distribution in z values, between $z=0.1$ and $z=2$. Magnitudes were generated from a Gaussian distribution with mean value $m(z)$ calculated using fiducial models. We have used our 50 points to simulate approximately 2000 SN by reducing their magnitude error by a factor $\sqrt{40}$ to 0.03 from the minimal 0.15 magnitude. Thus each generated point corresponds to 40 SNAP-like points, binned together. This corresponds to 1.4% relative error in d_L . Hence, our analysis is based on a SN search more extensive than the actual SNAP proposal. To obtain a quantitative estimate of how well models are resolved, we use one of two procedures. First, we can find the maximum likelihood contours of the various models for each of the fiducial models and explore the degeneracy in parameter space. Alternatively, we can assume that all models which predict $d_L(z)$ within 1% of the fiducial cosmological model for all z between 0 and 2 are deemed indistinguishable. We find that both approaches give comparable results. That is, the 95% C.L. likelihood contours using the first procedure are roughly equivalent to the indistinguishability region of the second.

II. DEPENDENCE OF LUMINOSITY DISTANCE ON DARK AND TOTAL EOS

Luminosity distance is defined to be the ratio of luminosity \mathcal{L} to flux \mathcal{F} :

$$d_L = \sqrt{\frac{\mathcal{L}}{4\pi\mathcal{F}}} = (1+z)r, \quad (1)$$

where the present value of the scale factor a_0 is normalized to unity (throughout subscript 0 denotes present values); r is the coordinate distance

$$r = \int_1^{1+z} \frac{dx}{H}; \quad (2)$$

and H is the Hubble parameter $H = \dot{a}/a$. The observed SN magnitudes are related to d_L ,

$$m(z) = M + 25 + 5 \log_{10}[H_0 d_L(z)], \quad (3)$$

M being the SN absolute magnitude.

For a flat universe with two energy sources, matter (including dark matter) and a dark Q component, there are two equivalent routes to computing d_L without assuming anything about the time dependence of w_Q . One way is to use the algebraic relation between the total energy density and the Hubble parameter H . Using conservation equations, the energy densities of the dark component ρ_Q and that of ordinary matter ρ_m are given by

$$\rho_Q(z) = (\rho_Q)_0 (1+z)^3 \exp\left[3 \int_1^{1+z} w_Q \frac{dx}{x}\right], \quad (4)$$

$$\rho_m(z) = (\rho_m)_0 (1+z)^3. \quad (5)$$

Since

$$\left(\frac{H}{H_0}\right)^2 = \frac{\rho_m + \rho_Q}{(\rho_m)_0 + (\rho_Q)_0} = \frac{g}{1+g} (1+z)^3 + \frac{(1+z)^3}{1+g} \exp\left[3 \int_1^{1+z} w_Q \frac{dx}{x}\right], \quad (6)$$

where g denotes the present ratio of matter to dark energy densities $g = (\Omega_m/\Omega_Q)_0$, H can be expressed as

$$H = H_0 (1+z)^{3/2} \left(\frac{g}{1+g} + \frac{1}{1+g} \exp\left[3 \int_1^{1+z} w_Q \frac{dx}{x}\right] \right)^{1/2}. \quad (7)$$

Substituting this into d_L gives

$$d_L = \frac{(1+z)}{H_0} (1+g)^{1/2} \int_1^{1+z} \frac{dx}{x^{3/2}} \times \left[g + \exp\left(3 \int_1^x w_Q(y) \frac{dy}{y}\right) \right]^{-1/2}. \quad (8)$$

An equivalent approach is to treat the sum of dark matter and the dark energy component as a single cosmic fluid with average equation of state $w_T(z) = \Omega_Q(z)w_Q(z)$, where

$$w_T(z) = \frac{w_Q}{1 + (\rho_m/\rho_Q)} = \frac{w_Q}{1 + g \exp\left[-3 \int_1^{1+z} w_Q(x) \frac{dx}{x}\right]}. \quad (9)$$

Since H^2 is proportional to the total energy density in the universe, it can be expressed in terms of w_T as follows:

$$\left(\frac{H}{H_0}\right)^2 = \exp\left[3 \int_1^{1+z} (1+w_T(x)) \frac{dx}{x}\right]. \quad (10)$$

Here we have used the conservation equation for the total energy density. Using Eq. (10) we can express d_L in terms of w_Q as follows:

$$\begin{aligned} d_L &= \frac{(1+z)}{H_0} \int_1^{1+z} dx \exp\left[-\frac{3}{2} \int_1^x (1+w_T(y)) \frac{dy}{y}\right] \\ &= \frac{(1+z)}{H_0} \int_1^{1+z} \frac{dx}{x^{3/2}} \\ &\quad \times \exp\left[-\frac{3}{2} \int_1^x \left(\frac{w_Q(y)}{1 + g \exp\left[-3 \int_1^y w_Q(u) \frac{du}{u}\right]} \right) \frac{dy}{y}\right]. \end{aligned} \quad (11)$$

This expression for d_L as a function of w_Q has one more integral than the relation in Eq. (8), but it is pedagogically useful in demonstrating that d_L is sensitive only to a weighted average of w_T or w_Q and not to their detailed time dependence.

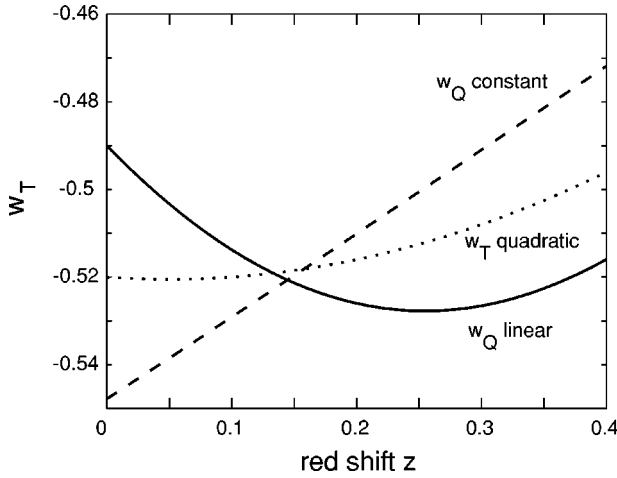


FIG. 1. $w_T(z)$ for three best fit models of three fits under three different assumptions: constant w_Q (dashed), linear w_Q (solid), and quadratic w_T (dotted), to data generated from a single fiducial model: $(w_Q, \Omega_m) = (-0.7 - 0.8z, 0.3)$. All fits prefer $w_T^* \equiv w_T(z^*) \approx 0.15) \approx -0.52$, but diverge for other values of z .

III. CONSTRAINING DARK AND TOTAL EOS USING SN MEASUREMENTS

Based on the previous sections, a number of lessons can be learned about measuring the EOS. First, the relation between w_T and d_L in Eq. (11) involves an integral, so we do expect some degeneracy in the determination of $w_T(z)$ from SN measurements. To determine the EOS of the dark energy itself, w_Q , the total energy density must be resolved into a matter component and a dark energy component. Hence, if Ω_m and Ω_Q are not known from independent measurements, determining w_Q entails an additional uncertainty. For example, consider a flat universe with $\Omega_T = \Omega_m + \Omega_Q = 1$. Since the matter EOS is $w_m = 0$, it follows that $w_T = w_Q \Omega_Q$. Two models with different values of w_Q may produce the same value of w_T and, consequently, d_L , due to offsetting differences in the value of Ω_m .

The more negative w_T is, the faster is the expansion. Therefore, a more negative (positive) w_T will make d_L larger (smaller). In addition, light from earlier times (emitted at higher z values) must pass through the low z universe to reach us. This means that changes in w_T at lower z affect d_L at higher z . The converse is not true. Changes in w_T at high z do not affect d_L at lower z .

Consequently, it is not surprising that SN measurements of d_L provide stronger constraints on $w_T(z)$ at low z than at high z . In particular, if all cosmic parameters other than $w_Q(z)$ are fixed, there is a particular, relatively low value of $z = z^*$ for which $w_T(z)$ is most tightly constrained. This value of z^* is clearly seen in our numerical results and was noted independently by [11,27]. For example, Fig. 1 shows the EOS $w_T(z)$ for three models each of which is obtained by best fit to $d_L(z)$ for a fiducial model $(w_Q, \Omega_m) = (-0.7 - 0.8z, 0.3)$ using one of three fitting assumptions: (1) that the dark EOS is constant; (2) that the dark EOS is linear $w_Q = w_0 + w_1 z$; and (3) that the total EOS is quadratic $w_T = A + Bz + Cz^2$. While the real degeneracy is stronger than

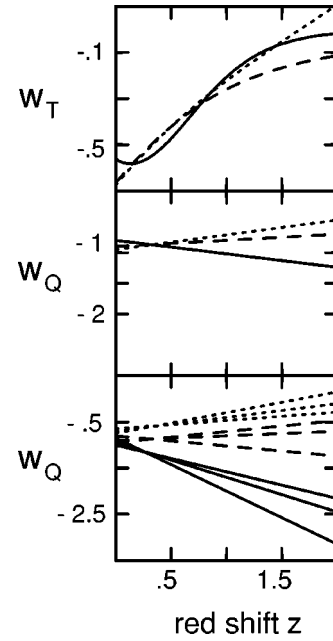


FIG. 2. Models within 95% C.L. region of a fit to data generated from the fiducial model $(w_Q, \Omega_m) = (-1, 0.3)$ assuming $w_Q = w_0 + w_1 z$. Top: The total EOS $w_T(z)$, for three different linear models. Middle: $w_Q(z)$ assuming $\Omega_m = 0.3$ exactly, for the same linear models. Bottom: $w_Q(z)$ for nine models, assuming that $0.2 < \Omega_m < 0.4$ (no relation between the dashed, dotted and solid lines of the bottom panel to those of the middle and top ones).

what is seen in the figure, we have chosen three examples to illustrate the existence of w_T^* and z^* . As can be seen, the fits disagree significantly for z far from $z^* = 0.15$, but all fits agree near z^* .

Unfortunately, the resolution of $w_Q(z^*)$, the quantity which most interests us, is degraded when we do not fix Ω_m but, instead, allow for the current uncertainty in its value. In Fig. 2, we show some linear fits to simulated data generated from the fiducial model $(w_Q, \Omega_m) = (-1, 0.3)$. The fits are representative examples which fit the fiducial model to within the 95% confidence region. The upper plot shows that $w_T(z)$ (with Ω_m fixed at 0.3) is relatively well resolved, and particularly well resolved at around redshift $z^* = 0.3$. The resolution is not that sharp in the middle plot which shows the corresponding w_Q , but a special point of enhanced resolution around $z = 0.4$ is still clearly seen. If one lets Ω_m vary in the realistic range of $0.2 - 0.4$, then w_Q becomes poorly resolved and the spread at z^* increases significantly. Similarly the spread in w^* and z^* increases significantly if more general functional forms of the EOS are considered.

We would like to stress that the constant or linear forms of w_Q that we use are not meant to be anything more than simple concrete examples to highlight the fact that we are dealing with a degenerate parameter space. Showing that if one assumes a linear $w_Q(z)$, then it can be resolved to, say, 50% does not logically mean that it can be measured to 50% accuracy generally since $w_Q(z)$ is resolved with different accuracy depending on its functional form. This can be illustrated with the following examples. In Fig. 3, the difference in magnitude (Δm) for models with various EOS is shown.

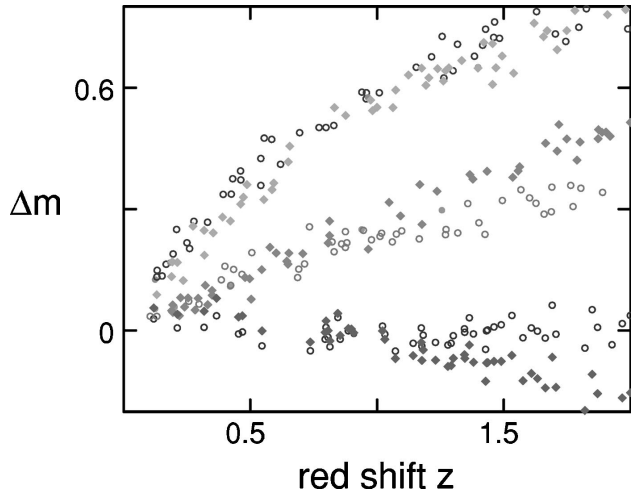


FIG. 3. Magnitude differences between pairs of degenerate models and a flat pure matter ($\Omega_m = 1$) universe. Each pair consists of simulated data points generated from one constant w_Q model (open circles) and one linear w_Q model with a large (positive or negative) derivative (full squares). The pairs are well separated but it is hard to separate between “members” of each pair. All models are flat and with fixed $\Omega_m = 0.3$. The specific models shown are somewhat extreme, and seem to diverge at high z , but they are statistically indistinguishable as shown in Fig. 2 of paper I.

There are three clusters of points, each of which corresponds to a simulation of SN data for a pair of different models. Each pair consists of a constant and linear w_Q . Each pair can be clearly separated from other pairs but the constant and linear “members” of a pair cannot be distinguished by SN data. The examples chosen for Fig. 3 have unrealistic large derivatives (of order unity) and therefore start to diverge from their constant partners for large z . More realistic examples with smaller derivatives or oscillatory behavior will be much harder to distinguish from a constant EOS.

Clearly the treatment of the SN analysis is important. If it is assumed that w_Q is constant, the figure shows that different values can be resolved to high accuracy, but if the as-

sumption of constancy is relaxed and a linear z dependence is allowed it becomes clear that the data can determine well only a single relation between w_0 and w_1 and that $w_Q(z)$ is poorly resolved.

The degree of degeneracy exhibited in the $w_Q = \text{const}$ fits depends on whether w_Q is positive or negative. Recall that if different models yield a total EOS $w_T = w_Q \Omega_Q$ that is approximately equal, they are degenerate, and therefore changes in w_Q can be compensated by changes in Ω_Q (or equivalently, in Ω_m). The difference between the case where w_Q is positive is due to the specific way in which this compensation mechanism operates. If w_Q is positive, the curvature of degeneracy lines in (w_Q, Ω_m) plane is positive, as shown in the right panel of Fig. 4 for a fiducial model with $w_Q = +0.5$. Conversely, if w_Q is negative, the curvature of the degeneracy line in (w_Q, Ω_m) plane is negative, as demonstrated in the left panel of Fig. 4. We have found that this result is unaffected by the value of the derivative of w_Q , even if it is quite large.

IV. COMMON PRACTICES AND PITFALLS IN DETERMINING $w_Q(z)$

The previous section (and paper I) show that the determination of $w_Q(z)$ from SN data is a more delicate process than it would seem. If we know *a priori* that w_Q is constant, then its value can be determined quite accurately. However, without this assumption, w_Q is poorly determined, and a larger (smaller) value for w_1 can be compensated with a smaller (larger) value of w_0 . Matters get much worse if Ω_m is uncertain: raising the value of both w_1 and w_0 can be compensated with a change in the value of Ω_m .

The analysis can be further confounded if certain common practices are followed. For example, many analyses assume that w_Q is constant and presume that, even if w_Q is time varying, the constant- w_Q fit will provide the mean value over recent epochs. Another common practice is to impose the condition that $w_Q(z)$ be limited to $-1 \leq w_Q(z) \leq 1$, based on the positivity and stability conditions that apply to most (but

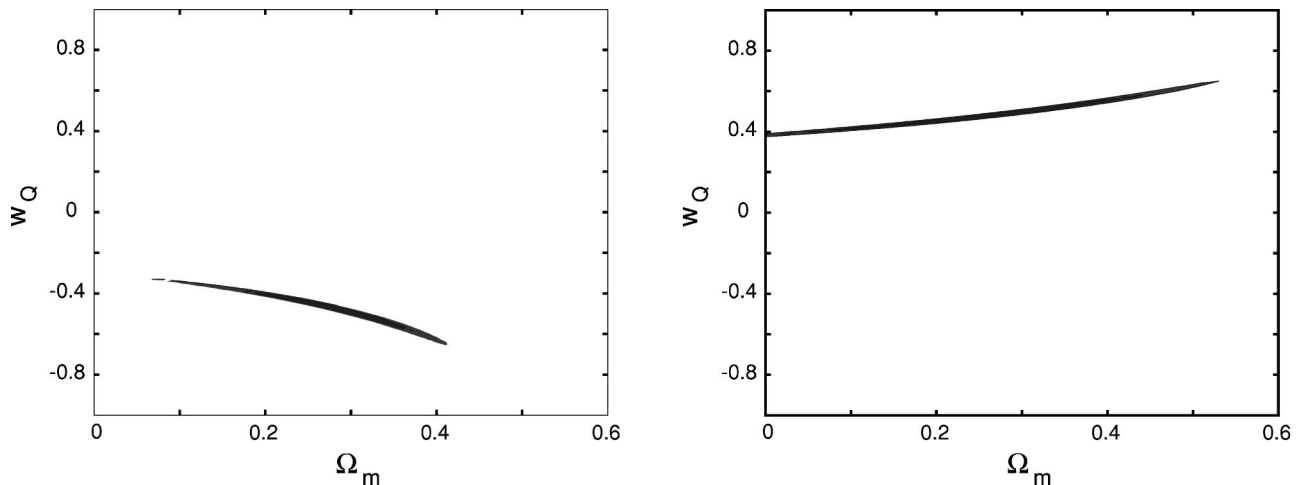


FIG. 4. 95% C.L. contours of fits to data generated from two fiducial models. The curvature of degeneracy contours is positive for a positive w_Q fiducial model (right) and negative for a negative w_Q fiducial model (left).

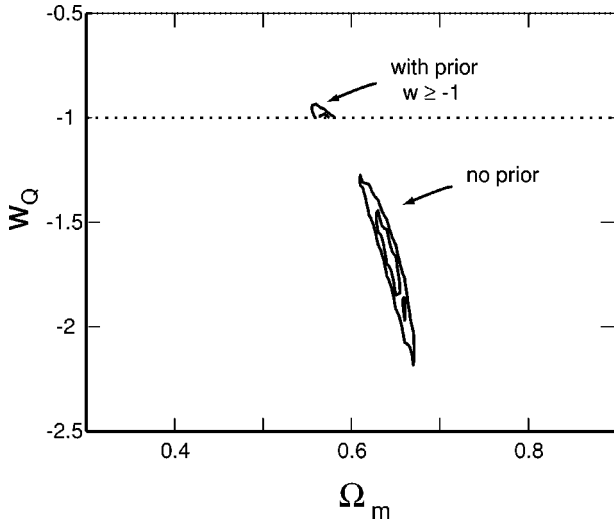


FIG. 5. Constrained (small) and unconstrained (larger and more negative) 68% and 95% confidence contours of a fit to data generated from a fiducial model with linear w_Q (w_Q, Ω_m) = $(-0.7 + 0.8z, 0.3)$. The fit is done under the (wrong) assumption that w_Q is constant. The example is somewhat extreme in that Ω_m shifts from 0.3 to 0.64, but in less extreme examples Ω_m stays within the range $0.2 < \Omega_m < 0.4$ and the best fit for w_Q is still negative and completely off from the actual $w_Q(z)$.

not all) forms of dark energy. We shall see that both practices can produce enormous distortions of the likelihood surface that lead to grossly incorrect conclusions.

For example, we have tried to fit data generated from a fiducial model with $w_Q = -0.7 + 0.8z$, and $\Omega_m = 0.3$ over a redshift range $0 < z < 2$. Note that the fiducial model has $w_Q > -1$ for all z . Yet, if we do a best-fit assuming that w_Q is constant, we find it to be $(w_Q, \Omega_m) \approx (-1.75, 0.65)$. Not only does the best fit have $w_Q < -1$, but the whole 95% confidence contour lies in a region where $w_Q < -1$. The results are the elongated contours in the lower part of Fig. 5. The reason for such a strange result can be understood from the functional dependence of d_L and w_Q . Assuming that $w_Q(z) = w_0 + w_1 z$, the energy density of the dark component is given in Eq. (4),

$$\rho_Q = (\rho_Q)_0 (1+z)^{3(w_0 - w_1 + 1)} \exp[3w_1 z], \quad (12)$$

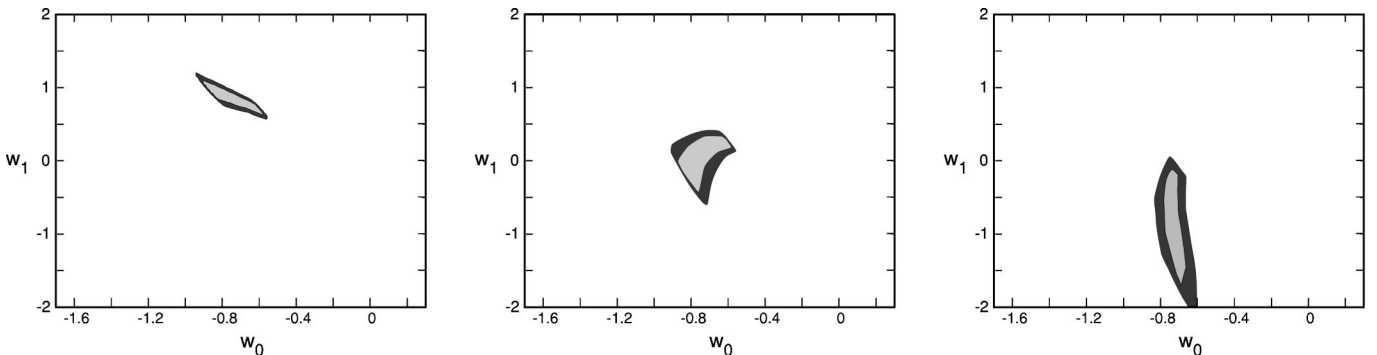


FIG. 6. Likelihood contours [68% (lighter) and 95% (darker) C.L.] in the (w_0, w_1) plane, for fits to data generated from 3 different fiducial models. Left: $(w_0, w_1, \Omega_m) = (-0.7, 0.8, 0.3)$. Middle: $(w_0, w_1, \Omega_m) = (-0.7, 0.2, 0.3)$. Right: $(w_0, w_1, \Omega_m) = (-0.7, -0.8, 0.3)$. Only the results shown in the left panel are inconsistent with a constant ($w_1 = 0$) w_Q model. In all fits Ω_m is marginalized over the range 0.2–0.4.

so decreasing both w_1 and w_0 has opposite and compensating effects, which tends to cancel each other's influence on d_L . The exponential factor determines the quantitative details of this compensation since changes in w_0 need to compensate also for changes in the exponential factor. It is therefore clear that the compensation cannot be perfect over a range of z 's. If we insist on the constant EOS (i.e., $w_1 = 0$), the fitting procedure will pick out a value of w_0 which is much more negative than the fiducial value. In the figure we have picked a fiducial with a large positive derivative to illustrate our point, but it is clear from our discussion that the same problem arises when time dependence is weaker, or in cases that the EOS has a more general functional form.

Introducing $w_Q > -1$ can give a very misleading impression of how well w_0 is resolved. For example, suppose that we assume that w_Q is constant and $w_Q > -1$, as is standard practice. The results are shown in Fig. 5, the small contours truncated at $w_Q = -1$. They seem to suggest that the data support the conclusion that $w_Q = -1$ with a high level of confidence. The best fit is $(w_Q, \Omega_m) \approx (-1, 0.58)$. Yet, this is not related in any obvious way to the fiducial model, $w_Q = -0.7 + 0.8z$ and $\Omega_m = 0.3$. The values of χ^2 per degree of freedom for the best fit models of Fig. 5 are reasonable: 0.95 for the unconstrained fit, and 1.39 for the constrained fit. So, what appears to be a compelling result is actually a total distortion. Of course, it is also conceivable that the actual $w_Q(z)$ is less than -1 , in which case the same procedure of introducing a prior would falsely suggest that $w = -1$ fits well.

V. ASYMMETRY IN DETERMINATION OF THE TIME DEPENDENCE OF THE DARK EOS

An EOS in which $w(z)$ has a large positive time derivative is easier to detect than one which has a large negative time derivative. In either case, the derivative must be large to be detected, as pointed out in paper I, but here we are demonstrating that the challenge is asymmetric. The point is illustrated in Fig. 6. The middle panel shows a fiducial model with a modest value of $w_1 = 0.2$, and, as can be seen, this case cannot be distinguished from a model in which $w_1 = 0$. That is, the 95% C.L. contours overlap the line $w_1 = 0$, corresponding to no time variation. The left and right panels

show cases in which $w_1=0.8$ and -0.8 , respectively. The contours for the $w_1=0.8$ case (left) lie far from the $w_1=0$ line, so the time variation is detectable in this example. On the other hand, the contours for the $w_1=-0.8$ case (right) overlay the $w_1=0$, so the time variation is not resolved.

This effect can be explained by considering the variation of the total average EOS w_T with respect to w_1 , $\Delta w_T = f(w_1)\Delta w_1$:

$$f(w_1) = \Omega_Q [z + 3w_Q(z - \ln(1+z))(1 - \Omega_Q)]. \quad (13)$$

We consider w_T because the measurements of d_L are directly sensitive to w_T , so that models can only be distinguished if they have different w_T . As can be seen from Eq. (13), w_T is much less sensitive to changes in w_1 when it is negative than when it is positive, mainly due to the value of Ω_Q being larger for positive values of w_1 . We conclude that, in order to detect that w_Q is time dependent, it must be that the time variation is large, roughly $w_1 > 0.5$, and it helps if w_1 is positive. This corresponds to the case where acceleration is becoming stronger as time evolves.

VI. COMBINING SUPERNOVAE WITH OTHER APPROACHES

Measurements to determine the EOS of the dark energy can be direct or indirect. Direct methods, such as SNIa observations, the Alcock-Paczynski (AP) test [32], and the cosmic microwave background (CMB) attempt to measure the Hubble parameter H , its derivative H' and Ω_m , or some function of them. Indirect methods, such as structure formation aspects of the CMB and measurements of large scale structure (LSS) try to infer $w_Q(z)$ from its effects on structure evolution.

An example of a complementary observation is the Alcock-Paczynski (AP) test. The physical transverse size of an object is given by $d_T = d_A \Delta\theta = [r/(1+z)]\Delta\theta$, d_A being the angular distance and $\Delta\theta$ the observed angular size. The physical radial size is $d_R = \int \sqrt{g_{rr}} dr = [1/(1+z)H(z)]\Delta z$. For a population of spherical objects, the AP test is given by equating the transverse and radial sizes: $AP(z) = \Delta z/\Delta\theta = H(z)r(z) = H(z)\int_1^{1+z} dx/H$.

The AP test on its own is not expected to improve the resolution of the dark EOS since it has a more complex dependence on w_Q than d_L . What does seem promising, as pointed out by McDonald [33,34], is that the AP test can further constrain the range of Ω_m .

Figure 7 shows the likelihood contours assuming optimistic anticipated errors over a continuous range between $z=0$ and $z=2$ of 1.4% for d_L , and, for the AP test, 50 bins between redshift $z=1.5$ and $z=3$ measured with 3% error per bin [34]. Both simulations represent highly optimistic assumptions about future measurements. The results are interesting. The better constraint on Ω_m from the AP test reduces the uncertainty in w_0 , but does not significantly change the uncertainty in the time variation, w_1 . This is not surprising since even a perfect determination of Ω_m would leave a considerable uncertainty in w_1 , as shown in paper I. To be sure, the Alcock-Paczynski test is useful and worth pursuing, and

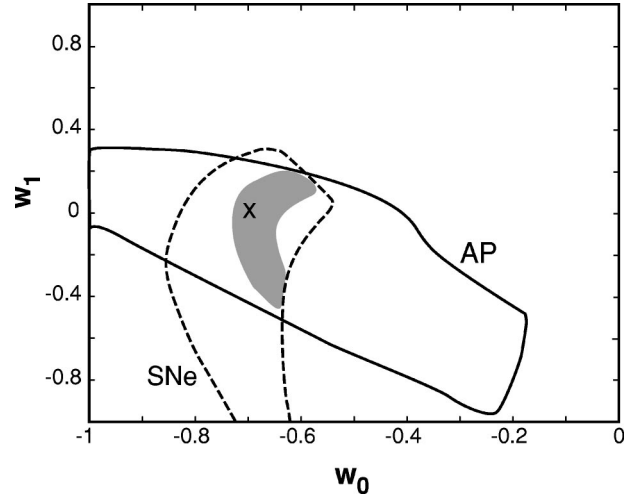


FIG. 7. Two-sigma contours in the $(w_0, w_1) \equiv (w_Q(z=0), dw_Q/dz_0)$ plane for two idealized experiments. One measures thousands of supernovae between $z=0$ and $z=2$ (dashed contours). The supernovae are divided into 50 bins with a net error of 1.4% per bin. The second experiment is an optimistic estimate for the AP test (solid contours), assuming 50 bins of Lyman-alpha clouds uniformly distributed between $z=1.5$ and $z=3$ with each bin measured with an accuracy of 3%. Both experiments assume a fiducial model with $\Omega_m=0.3$, $\Omega_Q=0.7$, $w_Q=-0.7=\text{const}$, indicated by the X. In both experiments Ω_m is marginalized over the range 0.2 to 0.4. The two-sigma joint likelihood for the two observations is shown in the shaded region.

a highly precise measurement combined with a highly precise measurement of SNe could determine the present value of w to within 15 or 20%. However, it does not help significantly with the particular problem of pinning down the time variation of the equation of state.

Measurements of the CMB anisotropy provide an additional probe of $w(z)$. This probe also suffers from a degeneracy problem, even in the case where w is constant. The positions of the acoustic peaks in the temperature anisotropy power spectrum depend on the angular distance (d_A) to the last scattering surface which, just like the luminosity distance for supernovae, depends on a multi-integral over $w(z)$, $d_A = d_L/(1+z)^2$. In addition, the heights of the peaks depend on Ω_Q and the Hubble parameter, $H_0 = h100$ km/parsec/sec. When all effects are considered, then, as shown by Huey *et al.* [35], the power spectrum is unchanged as certain combinations of Ω_m , h , and w are varied. Consequently, none of these parameters can be determined well by the CMB data alone. Instead, measurements can only constrain these parameters to a thin two-dimensional surface in this three-dimensional parameter subspace.

The reason why one might be optimistic about combining CMB anisotropy and SN measurements is that the degeneracy surface for the CMB anisotropy measurements is nearly orthogonal to the degeneracy surface for the SN measurements for the case of constant w . Figure 8 illustrates the small overlap between the SN and CMB degeneracy regions in the Ω_m - w plane. Other authors have considered adding the CMB contribution [27,28] but they have not included the

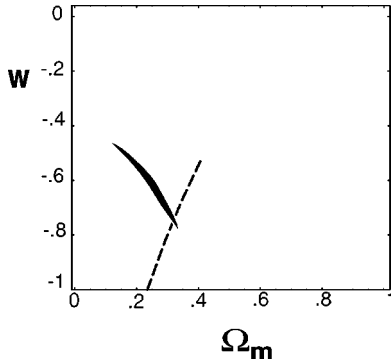


FIG. 8. A simulation of the problem that arises if one assumes $w(z)$ is constant in the fitting procedure. For a given fiducial model, the likelihood fit for the CMB anisotropy (dashed line) and SN luminosity distance-redshift (contour) observations are illustrated. The degeneracy curve for the CMB assumes cosmic variance limited sampling, and the SN contour assumes 1% error in luminosity distance. Each degeneracy region is long and thin, and the two are nearly orthogonal. Based on the small overlap, one is tempted to conclude that constancy of w is well established and its value is well determined. However, that conclusion is absolutely wrong. The fiducial model in this example actually has a rapidly time-varying $w(z) = -2/3 - 1/6z$ for $z < 2$ and $w(z) = -1$ for $z > 2$. The degeneracy regions were computed assuming $w_1 = 0$, but, if w_1 is fixed at a value somewhat less than zero, say, there are once again two narrow degeneracy regions which intersect over a small region, but the value of w_0 in the overlap region is significantly shifted. That is, the two experiments produce two degeneracy surfaces that intersect along a curve in the w_1 direction along which a degeneracy remains.

degeneracy aspect. As we shall show below, introducing time-varying $w(z)$ introduces additional degeneracy that spoils the resolution even when the SN and CMB anisotropy measurements are combined.

Rather than do another complete survey, which is a major technical challenge on its own, we illustrate the degeneracy in parameter space with a simple example in which we consider the family of $w(z)$ of the form

$$\begin{aligned} w(z) &= w_0 + w_1 z & \text{for } z < 2 \\ &= w_0 + 2w_1 & \text{for } z \geq 2. \end{aligned} \quad (14)$$

This form was chosen to allow significant time variation recently when Ω_Q is large and, in particular, to be similar to the models considered in paper I for $z < 2$. For $z < 2$, the degeneracy problem with respect to SN data was already demonstrated and the w_0 - w_1 degeneracy region was characterized. However, we could not simply maintain the linear change in $w(z)$ with respect to z out to the last scattering surface at $z = 1000$ because the value of w would be ridiculously nonphysical. Hence, we cut off the z dependence at a value of z where Ω_Q is negligible and $w(z)$ is physically plausible. We then maintain that condition back to the last scattering surface. For example, for $w = -2/3 - 1/6z$ and $(\Omega_Q)_0 = 0.7$, at $z = 2$ the dark energy contribution to the total energy density is less than 15%, which makes the details of

the z -dependence cutoff unimportant. From $z = 2$ until the last scattering surface, this model will have $w = -1$.

The value of w_0 in our time-varying examples is fixed to be $-2/3$ except where otherwise stated. In each of these models, we also have $h = 0.65$, $\Omega_Q = 0.7$, $\Omega_m = 0.3$, and $\Omega_b = 0.04$. Here Ω_b is the baryon density and Ω_m is the total matter density (baryonic plus nonbaryonic). Note that luminosity distance-redshift measurements are not sensitive to Ω_b/Ω_m , but the CMB measurements are.

The time-varying models were treated as the fiducial model, and then a numerical search was performed for a constant EOS model that is indistinguishable from the fiducial model based on the combined measurement of the CMB and of supernovae. Models were considered degenerate under the combined tests if (1) the percent difference between the luminosity distance-redshift predictions for the two models is less than one percent out to $z = 2$ (the same criterion as in paper I); and (2) the CMB predictions for the two models assuming a full-sky cosmic-variance limited measurement (no experimental error) cannot be distinguished to better than 3σ . Both criteria are based on optimistic predictions of what will be realistically possible.

For the CMB, distinguishability between a model with a constant w and a fiducial with a time-dependent w was determined by a log-likelihood analysis. The log-likelihood was calculated according to the log-likelihood formula obtained by Huey *et al.* [35]:

$$\mathcal{L}_{FC} = - \sum_l \left(l + \frac{1}{2} \right) \left(1 - \frac{C_l^{(F)}}{C_l^{(C)}} + \log \frac{C_l^{(F)}}{C_l^{(C)}} \right). \quad (15)$$

The coefficients $C_l^{(F)}$ and $C_l^{(C)}$ are the CMB multiple moments corresponding to the fiducial and constant equation of state models, respectively.

Figure 8 illustrates the problem that arises if one assumes $w(z)$ is constant in the fitting procedure. We have already observed that this distorts results for the case of SN data alone. Here we show that the problem remains if CMB data is co-added. Assuming w is constant ($w_1 = 0$), both measurements produce a thin degeneracy region in the Ω_m - w plane. Based on the small overlap, one is tempted to conclude that constancy of w is well established and its value is well determined. However, this conclusion is absolutely wrong. In this example, the fiducial model actually has a rapidly time-varying EOS $w(z) = -2/3 - 1/6z$ for $z < 2$ (which produces a change in w of 50% over this range), and $w(z) = -1$ for $z > 2$. The degeneracy regions were computed assuming $w_1 = 0$. If w_1 were to be fixed at a different value, once again the two measurements will give two narrow degeneracy regions with a small overlap, but the value of w_0 in this overlap region is significantly shifted. For example, as shown in Fig. 8, fixing $w_1 = 0$ results in $w_0 = -0.74$ with a few percent error. However, if w_1 were to be fixed at its correct value $w_1 = -1/6$, the result would have been $w_0 = -2/3$, again with a few percent error. But the central values differ by more than 10%. It is clear, then, that the two measurements produce two degeneracy surfaces which intersect along a degenerate curve which passes through a range of models with

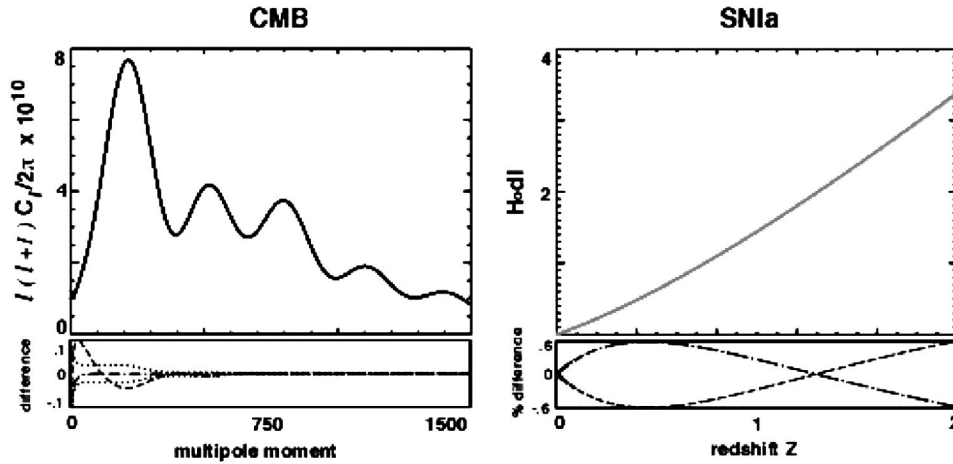


FIG. 9. Illustration of the degeneracy problem for a model with constant w and two models with time-varying w as discussed in the text. The upper left hand panel compares the CMB power spectra. The lower left shows the differences between the time-varying models and the constant w model and shows that they are less than or comparable to the full-sky cosmic variance theoretical uncertainty, the envelope shown in the figure (dotted lines). The upper right panel compares predictions for the luminosity distance-redshift relation. The lower right panel shows the differences with respect to a constant model are less than the 1% resolution anticipated from supernovae measurements.

varying values for w_0 and w_1 , that remain degenerate under the combined observations. For more complicated functional forms of $w_Q(z)$ the degeneracy curve becomes a more complicated higher dimensional surface, and the range of degeneracy in parameter space (say, for w_0) increases.

The complications in the process of extracting the EOS from both measurements are further illustrated in Fig. 9. There we show two time-varying models with slopes $|w_1| > 0.1$, one of which is degenerate (by the log-likelihood test) with a constant w model with $w = w_0 = -0.72$ and $\Omega_b = 0.04$, $\Omega_m = 0.31$, $\Omega_Q = 0.69$, and $h = 0.64$. The other can be barely resolved making the most optimistic estimates about cosmic variance. A slight decrease in w_1 , or a slight decrease in experimental sensitivity would render the second model degenerate. The lower two plots magnify the differences between the predictions of the models. For the case of the CMB, we have also shown the envelope based on the constant w model corresponding to the full-sky cosmic variance limit. For the SN, we have constrained the limits to lie between $\pm 1\%$.

If $|w_1|$ is larger than $1/6$ for our particular form of $w(z)$, we find that there is no overlap between the degeneracy curve picked out by CMB measurements and the degeneracy contour picked out by SN measurements (where both fit assuming w is constant). An example is shown in Fig. 10. In the case of negative (positive) w_1 the CMB measurements that fit best suggest low (high) Ω_m whereas the SN measurements suggest high (low) Ω_m . If this absence of overlap were to be found in the real data, an interpretation to pursue is that w is rapidly time varying. Yet such an extreme scenario is not favored by most theoretical models, most of which predict a moderately time-varying w . For the more likely case, in which the two measurements do overlap, combining them reduces degeneracy by only a modest amount, generally not even enough to decide whether the dark energy in the universe has a time varying equation of state or not.

Coadding the CMB to the SN data represents an improve-

ment in the sense that w_1 and w_0 are more constrained than with SN data alone based on our earlier analysis or in paper I. The improvement is by a factor of four or so *assuming a linear form for $w(z)$* , which is significant. However, there remains a large uncertainty in the EOS. Furthermore, we would stress once again that the accuracy in determining w strongly depends on its assumed functional form. The range of degeneracy obtained for w_1 (a bit more than ± 0.1) in our example underestimates the degeneracy for general $w(z)$. For example, for parabolic forms, the uncertainty in w_1 blows up to ± 0.5 . Given the extraordinarily precise data that has been brought to bear, the allowed variation in w_0 , w_1 , and Ω_m is disappointing.

VII. CONCLUSIONS

An important challenge for observational cosmology is to measure the equation of state of the dark energy, $w_Q(z)$. This

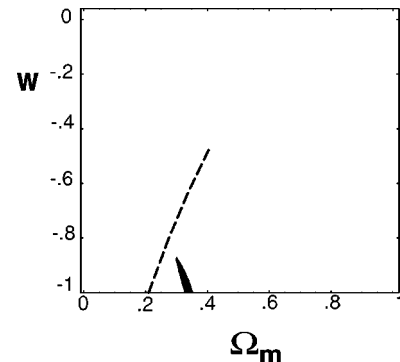


FIG. 10. The same as Fig. 8 but with a fiducial model with $w_1 = 1/3$. For cases like this with very rapid time variation in w , a symptom is that the CMB and SN degeneracy regions do not overlap. For w_1 large and positive, as in this example, the SN contour (solid black) lies to the right of the very thin CMB degeneracy region (dashed curve). For w_1 large and negative, the SN contour lies to the left.

can provide important information about the fundamental physics that is responsible for the accelerated expansion of the universe. Measurements of the distance-redshift relation using supernovae, perhaps combined with other direct methods such as the Alcock-Paczynski test or the cosmic microwave background, would appear to be promising methods. Indeed, analyses based on the *a priori* assumption that $w_Q(z)$ is constant suggest that w_Q can be resolved to 5% accuracy or better.

In this paper and paper I, though, we have uncovered a number of problems and pitfalls that arise when trying to determine $w_Q(z)$ without making prior assumptions. Our lessons may be summarized as follows.

Because measures of luminosity or angular distance depend on integrals over $w_Q(z)$, a first degeneracy problem arises in which neither the current value nor its time variation can be resolved to any useful accuracy (Sec. II).

Since the effect of dark energy on the luminosity distance depends on the combination $w_Q\Omega_Q$ rather than w_Q itself, a second degeneracy problem arises in which w_Q and Ω_Q are changed simultaneously so as to keep $w_Q\Omega_Q$ fixed (Sec. III).

Although SN measurements may extend to $z=2$, they are most sensitive to the behavior of $w_Q(z)$ at a modest value of $z^*\approx 0.1-0.4$ (Sec. III).

Consequently, if there were only the first degeneracy problem, $w_Q(z)$ could be well resolved at $z=z^*$ even though it is not well resolved for other values of z . Unfortunately, the resolution of $w_Q(z^*)$ is totally degraded when one includes uncertainty in Ω_Q and the second degeneracy problem (Sec. III, especially Fig. 2).

The common practice of fitting data assuming that $w_Q(z)$ is constant can lead to grossly distorted results. Similarly, the common practice of assuming $w_Q\geq -1$ can lead to grossly distorted results. Figure 5 shows a dramatic example in which these practices lead to the conclusion that $w_Q=-1$ and is well resolved when, in reality, $w_Q>-1$ and rapidly increasing (Sec. IV).

Time variation of w_Q is more easily detected if $w_Q(z)$ is an increasing function of z rather than decreasing (Sec. V).

To resolve $w_Q(z)$ with supernova data, an additional test is needed. Given optimistic estimates of experimental uncertainties, the Alcock-Paczynski test combined with the supernovae measurements can constraint the current value of w to within 20% or so. However, neither the Alcock-Paczynski test nor microwave background anisotropy measurements

provide the needed resolution to constrain the time variation (Sec. VI).

Our principal conclusion is that a new test is required to achieve the goal of measuring $w_Q(z)$. In devising a new test, the two considerations must be precision and model dependent. Thus far, among the measurements that we have considered, the measurements which are precise give constraints on w_Q that are highly model dependent, leading to degeneracy problems. Tests which are not model dependent turn out to be difficult to measure precisely. So, there lies the challenge.

In considering alternatives, it is critical to include practical estimates of their uncertainties. Furthermore, one must consider how the new tests themselves depend on $w_Q(z)$. For example, claims have been made that Ω_m and Ω_Q have been or will be measured very accurately by measurements of the cosmic microwave background [36]. However, those estimates are based on assuming that $w_Q=-1$. Making no prior assumption about $w_Q(z)$, a degeneracy problem once again arises [35] that spoils the resolution of Ω_Q and $w_Q(z)$, as discussed in Sec. VI.

While trying to devise a new test to determine w_Q , it is worth mentioning that a precise measurement of H' will be extremely useful. The dependence of w_Q on H , H' (prime denotes a derivative with respect to $x=1+z$) and Ω_m is given by $w_Q=(\frac{2}{3}xHH'-H^2)/(H^2-\Omega_mH_0^2x^3)$. A good measurement of H' is clearly crucial to the resolution of w_Q , but current tests do not probe H' directly. The next best option is to measure $H(z)$, and then estimate H' by calculating its derivative. Obviously, this worsens the resolution for H' and increases the uncertainty in w_Q .

Three additional approaches that we have not tried yet are measuring the time dependence of structure growth on $w(z)$ [37], gravitational lensing, and direct measurements of dz/dt (to be discussed elsewhere [38]).

ACKNOWLEDGMENTS

We thank A. Albrecht, G. Efstathiou, D. Eichler, P. McDonald, and B. Paczynski for helpful comments, E. Linder for helpful comments on a previous version of the manuscript, and D. Oaknin for valuable programming assistance. This research was supported by grant No. 1999071 from the United States-Israel Binational Science Foundation (BSF) (I.M. and R.B.) and by the US Department of Energy grant DE-FG02-91ER40671 (J.M. and P.J.S.).

[1] S. Perlmutter *et al.*, *Astrophys. J.* **517**, 565 (1999).
 [2] A. G. Riess *et al.*, *Astrophys. J.* **116**, 1009 (1998).
 [3] S. Perlmutter, M. S. Turner, and M. White, *Phys. Rev. Lett.* **83**, 670 (1999); P. Garnavich *et al.*, *Astrophys. J.* **509**, 74 (1998).
 [4] See, for example, J. P. Ostriker and P. J. Steinhardt, *Nature (London)* **377**, 600 (1995); L. M. Krauss and M. S. Turner, *Gen. Relativ. Gravit.* **27**, 1137 (1995).
 [5] See, for example, N. Bahcall, J. P. Ostriker, S. Perlmutter, and P. J. Steinhardt, *Science* **284**, 1481 (1999) and references therein.

[6] R. R. Caldwell, R. Dave, and P. J. Steinhardt, *Phys. Rev. Lett.* **80**, 1582 (1998).
 [7] I. Maor, R. Brustein, and P. J. Steinhardt, *Phys. Rev. Lett.* **86**, 6 (2001).
 [8] N. Weiss, *Phys. Lett. B* **197**, 42 (1987); B. Ratra and J. P. E. Peebles, *Astrophys. J. Lett. Ed.* **325**, L17 (1988); C. Wetterich, *Nucl. Phys.* **B302**, 668 (1988); *Astron. Astrophys.* **301**, 32 (1995); J. A. Frieman *et al.*, *Phys. Rev. Lett.* **75**, 2077 (1995); K. Coble, S. Dodelson, and J. Frieman, *Phys. Rev. D* **55**, 1851 (1997); P. G. Ferreira and M. Joyce, *Phys. Rev. Lett.* **79**, 4740

- (1997); Phys. Rev. D **58**, 023503 (1998); C. Armendariz-Picon, V. Mukhanov, and P. J. Steinhardt, Phys. Rev. Lett. **85**, 4438 (2000).
- [9] G. Efstathiou, Mon. Not. R. Astron. Soc. **310**, 842 (1999).
- [10] S. Podariu, P. Nugent, and B. Ratra, Astrophys. J. **553**, 39 (2001).
- [11] P. Astier, astro-ph/0008306.
- [12] J. Weller and A. Albrecht, Phys. Rev. Lett. **86**, 1939 (2001).
- [13] T. Chiba and T. Nakamura, Phys. Rev. D **62**, 121301 (2000).
- [14] V. Barger and D. Marfatia, Phys. Lett. B **498**, 67 (2001).
- [15] M. Chevallier and D. Polarski, Int. J. Mod. Phys. D **10**, 213 (2001).
- [16] M. Goliath, R. Amanullah, P. Astier, A. Goobar, and R. Pain, astro-ph/0104009.
- [17] N. Trentham, astro-ph/0105404.
- [18] E. H. Gudmundsson and G. Bjornsson, Astrophys. J. **565**, 1 (2002).
- [19] J. Weller and A. Albrecht, Phys. Rev. D **65**, 103512 (2002).
- [20] S. C. Ng and D. L. Wiltshire, Phys. Rev. D **64**, 123519 (2001).
- [21] E. Linder, astro-ph/0108280.
- [22] Jens Kujat, Angela M. Linn, Robert J. Scherrer, and David H. Weinberg, astro-ph/0112221.
- [23] D. Huterer and M. S. Turner, Phys. Rev. D **60**, 081301 (1999).
- [24] T. D. Saini, S. Raychaudhury, V. Sahni, and A. A. Starobinsky, Phys. Rev. Lett. **85**, 1162 (2000).
- [25] B. Boisseau, G. Esposito-Farese, D. Polarski, and A. A. Starobinsky, Phys. Rev. Lett. **85**, 2236 (2000).
- [26] Y. Wang and P. M. Garnavich, Astrophys. J. **552**, 445 (2001).
- [27] D. Huterer and M. S. Turner, Phys. Rev. D **64**, 123527 (2001).
- [28] M. Tegmark, astro-ph/0101354.
- [29] P. S. Corasaniti and E. J. Copeland, Phys. Rev. D **65**, 043004 (2002).
- [30] Y. Wang and G. Lovelace, Astrophys. J. Lett. **562**, L115 (2001).
- [31] An example is the proposed SNAP (Supernova Acceleration Probe) satellite, <http://snap.lbl.gov>
- [32] C. Alcock and B. Paczynski, Nature (London) **281**, 358 (1979).
- [33] P. McDonald and J. Miralda-Escude, Astrophys. J. **518**, 24 (1999).
- [34] P. McDonald, astro-ph/0108064.
- [35] G. Huey, L. Wang, R. Dave, R. R. Caldwell, and P. J. Steinhardt, Phys. Rev. D **59**, 063005 (1999).
- [36] M. S. Turner, astro-ph/0106035.
- [37] J. Weller, R. Battye, and R. Kneissl, astro-ph/0110353.
- [38] D. Wesley, A. Loeb, and P. J. Steinhardt (unpublished).